July 4–8, 2021, Évora, Portugal

Detection of Leek Rust and White Tip Disease Under Field Conditions Using Hyperspectral Proximal Sensing and Supervised Machine Learning

Appeltans Simon [a], Pieters Jan[b] , Mouazen Abdul M.[a,*]

[a] Department of Environment, Faculty of Bioscience Engineering, Ghent University, 9000 Ghent, Belgium

[b] Department of Plants and crops, Faculty of Bioscience Engineering, Ghent University, 9000 Ghent, Belgium

* Corresponding author. Email: Abdul.Mouazen@UGent.be

Abstract

Crop diseases remain one of the key yield-limiting factors in leek production, causing the need for continuous fungicide applications, resulting in socio-economic and environmental costs. Precision agriculture aims at reducing these costs, while maintaining or improving farmer revenues. The first requirement for the implementation of variable rate fungicide application is in-field measurement of the spread of disease. In this work, a disease detection methodology was created that could detect early stages of disease development in field conditions for two main diseases: leek rust and white tip disease. A hyperspectral training library was constructed for both diseases separately, containing spectra corresponding to healthy leek, weed plants, diseased leek plants and soil. A custom preprocessing and soil pixel removal strategy was constructed for each disease. An evaluation of 11 common classifiers was performed, of which a logistic regression classifier provided the highest classification accuracy. This logistic regression supervised machine learning classifier was then trained on the hyperspectral library. For leek rust disease, the focus was on detecting early infection (i.e. single rust pustules). For white tip disease, the model was used to classify the data into four classes: healthy plant material, early (pre-visual) disease, moderate disease, severe disease and fully developed disease. The overall accuracy of the disease model was 98.14% for rust and 96.74% for white tip disease. It can be concluded that the results in this work are an important step towards the mapping of leek rust and white tip disease, and that future research is needed to overcome certain challenges before variable rate fungicide applications can be adopted against leek diseases.template is designed to assist a high quality proceedings book editing and printing.

Keywords: Hyperspectral, Disease Detection, Leek White Tip Disease, Leek Rust Disease, Machine learning.

1. Introduction

Despite modern crop protection strategies, crop diseases remain one of the most important yield and revenue limiting factors in crop production. For leek (*Allium porri*), rust (*Puccinia allii* Rud) and white tip disease (*Phytophthora porri* Foister) cause economic losses due to cosmetic damage, yield reduction and secondary infections (Bart Declercq et al. 2012). This leads farmers to apply regular fungicide treatments once every 1 to 5 weeks to prevent disease incidence. However, these fungicides are costly and put a strain on the environment (Geiger et al. 2010). To deal with the economic and environmental costs associated with crop protection, researchers have developed the principles of precision agriculture. Using precision agriculture, farmers aim to apply the right amount of inputs, in the right place at the right time (Archbold Taylor et al. 2019; Anne-Katrin Mahlein 2016; Nawar et al. 2017). This, in theory, leads to lower operational costs while maintaining or even increasing yields and thus improving revenues. In addition to being profitable, this strategy also aims at reducing the environmental impact of agriculture.

Despite the recent surge in research on precision agriculture, its basic principles have been in practice for many years in leek cultivation, dating back to 1995 (P. D. de Jong, Daamen, and Rabbinge 1995). Farmers at the time mainly relied on visual inspection of the field, after which they could decide to apply full-field fungicides or focus the application on specific areas. Because this method is too laborious for modern crop protection, scientists are looking towards automating disease detection (Zhang et al. 2019; Behmann et al. 2015). Among the most promising novel technologies for disease detection are hyperspectral sensors (Grisham, Johnson, and Zimba 2010; Zhang et al. 2012; Anne-Katrin Mahlein 2016; Zhang et al. 2019). These sensors are able to provide fast, high quality reflectance measurements in dozens up to hundreds of wavebands in the visible (VIS) and near-infrared (NIR) spectrum, making them suited for early disease detection and mapping. However, to the best of our knowledge, no work has been published regarding the detection of leek diseases. Most authors in literature have instead focused on developing resistant cultivars and effective fungicides (Clarkson et al. 1997; P. D. de Jong, Daamen, and Rabbinge 1995; Doherty and Preece 1978; Jennings, Ford-lloyd, and Butler 1990; Smith et al. 2000; Theunissen and Schelling 1996).

The aim of the current work is to introduce and validate a novel method of detecting rust and white tip disease in field conditions using hyperspectral imaging machine learning. It will provide the first step towards mapping the spread of the named diseases throughout the field, to be used as input for applying variable rate fungicides.

2. Materials and Methods

2.1. Test field

The first measurement site was the experimental field of the 'Provinciaal Proefcentrum voor de Groenteteelt Oost-Vlaanderen' (PCG), Kruishoutem (Kruisem), Belgium, with coordinates of 50° 56' 40.3404" N, 3° 31' 26.4108" E. This field was used by the experimental centre to conduct a) a leek rust fungicide trial, whereby the Lucretius cultivar was cultivated under normal farming conditions and the efficacy of a range of fungicides was assessed by comparing levels of naturally occurring infection under different spraying regimes, and b) a leek white tip disease sensitivity trial for several cultivars by comparing levels of naturally occurring infection. Leek plants were planted in ridges with a width of 0.65 m and a within row distance of 0.10 m, with four ridges per crop row. Plots were delineated with a length of 2.5 m per plot (Figure 1). Measurements were taken in December 2018 and in February 2019. Data was measured at 6 points along the crop row for leek rust disease, and 5 points for leek phytophthora disease (Figure 1), scanning in the direction perpendicular to the crop row (Figure 1, A). The soil type in this field was loamy sand, with a relatively dark colour.

The second data collection site was the Bottelare experimental farm (Merelbeke, Belgium) of Ghent University and Ghent University College with coordinates of 50°57'45.2"N, 3°45'36.3"E. The soil type in Bottelare consisted of a sandy loam, with a reddish-brown colour. Leek plants of cultivar Pluston were pre-germinated and grown in pots, then transplanted to the field in ridges with a width of 0.75 m, height of 0.30 m and within-row distance of 0.12 m. The field was divided into plots of 3 by 3 m and inoculated on March 18th 2019. The inoculation consisted of four treatments: rust disease, leek white tip disease, both diseases simultaneously and a healthy control, with a total of 16 plots in a randomized block design. Since the first inoculation proved unsuccessful, a second inoculation attempt was performed on April 4th 2019, which was relatively successful. Still, disease pressure in the Bottelare experimental field remained below a few plants infected per plot. Measurements were taken at one-week intervals between March 2019 and May 2019, along the middle two crop rows of each plot (Figure 1, B).

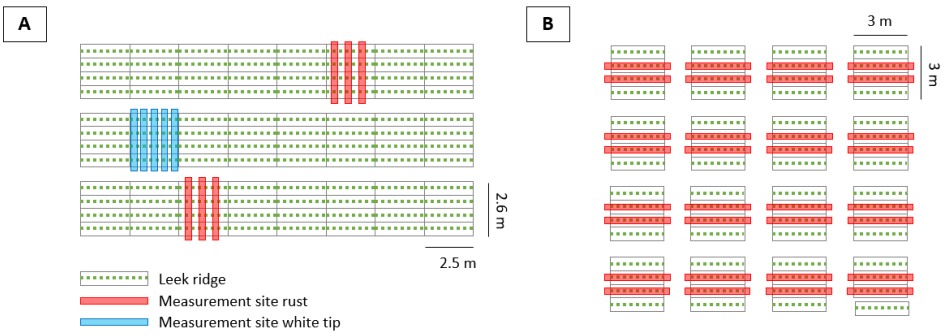

Figure 1: measurement sites at the (A) "Provinciaal Proefcentrum voor de Groenteteelt Oost-Vlaanderen" (PCG) and (B) Bottelare experimental farm.

3.2 Visual assessment of disease severity

Five measurement sites were selected based on the presence of white tip disease in the field at the PCG experimental centre (Figure 1). The level of infection was assessed by technical staff at the centre following the EPPO PP 1/120(2) – guideline on 28/01/2019 and 28/02/2019, showing disease pressures of 1.44% on the first and 2.84 % on the second measurement day. For the Bottelare experimental farm, the disease pressure was too low to be assessed following the EPPO protocol. The methodology described in Clarkson et al. (1997) was therefore followed, by which individual leaves can be assessed for disease severity (Clarkson et al. 1997). The low infection rate was likely due to the weather conditions, which were unusually dry for the time of year and is known to limit infection (Bart Declercq et al. 2012). Most plants in the Bottelare dataset contained zero lesions, with some plants showing signs of early white tip infection (less than 5 lesions per plant).

Six measurement sites were selected based on the presence of rust disease in the field at the PCG experimental centre (Figure 1). The level of infection was assessed by technical staff at the centre following the EPPO PP 1/120(2) guideline on 20/11/2018, showing 0.84% in one plot and 10.32% in the second plot. For the Bottelare experimental farm, the disease pressure was too low to be assessed following the EPPO protocol, so the protocol described in Clarkson et al. (1997) was followed (Clarkson et al. 1997). Most plants contained zero rust pustules, but there was some early disease development with some plants showing 0-10 rust pustules on average.

2.2. Sensor setup

The sensor setup used in these experiments is described in detail in Appeltans et al. (2020) (Appeltans et al. 2020). Hyperspectral data was collected using an FX10e pushbroom sensor (Specim, Finland) from a proximal perspective (0.30 m above crop canopy), measuring reflectance in 224 bands between 400 and 1000 nm with an integration time of 1 ms.

2.3. Hyperspectral library building

To build the hyperspectral library, the methodology of Xie et al. (2015) was followed in which regions of interest were visually identified containing healthy, diseased and background pixels (Xie et al. 2015). Then, the spectra belonging to these pixels were labelled

and exported into separate datasets using ENVI software (Harris Geospatial, USA). The final composition of each training set was 7,436 spectra for each class of the white tip disease model (white tip disease, healthy leek crops both shaded and unshaded, weeds and soil), leading to a total training library of 29,744 spectra, and 10,854 spectra for each class of the leek rust disease model (rust disease, healthy leek crops both shaded and unshaded, weeds and soil), leading to a total training library of 43,416 spectra.

2.4. Preprocessing and model selection

Using the hyperspectral training library, an iterative process was started in which the optimal combination of preprocessing, feature selection and model selection was determined (Figure 2). 11 classifiers were examined using standard and slightly altered parameter settings, including K-nearest neighbors, support vector machine, gaussian process, decision tree, random forest, multilinear perceptron, AdaBoost, gaussianNB, logistic regression, linear discriminant analysis (LDA) and quadratic discriminant analysis (Pedregosa et al. 2011). These classifiers were combined with a variety of preprocessing techniques, including Savitzky-Golay smoothing, normalisation, derivation and feature selection. SelectKBest and SelectFromModel feature selection algorithms were tested (scikit-learn package), but they suffered from high correlation of neighbouring bands (Pedregosa et al. 2011). To solve this, these algorithms were used per region of the spectrum separately, to determine the optimal features for each spectral region of interest. Other dimensionality reduction strategies were tested, including principle component analysis (PCA), LDA, decision tree feature selection, support vector machine feature selection, selection based on highest variance, and visual identification of interesting spectral features.

The first step in the modelling cycle was white/dark reference correction, using a calibrated white reference target (SphereOptics, Germany, Alucore reflectance target, 500 × 500 mm, 95% reflectance). After selecting a combination of smoothing, derivation and normalisation, the data was fed to each of the classifiers. 70% of the dataset was used for model training, while 30% was used for model validation. The highest performing models were retained and used to classify images with known rust or white tip disease infection. Misclassified pixels were examined, and the preprocessing was altered based on the spectral characteristics of these misclassified spectra.

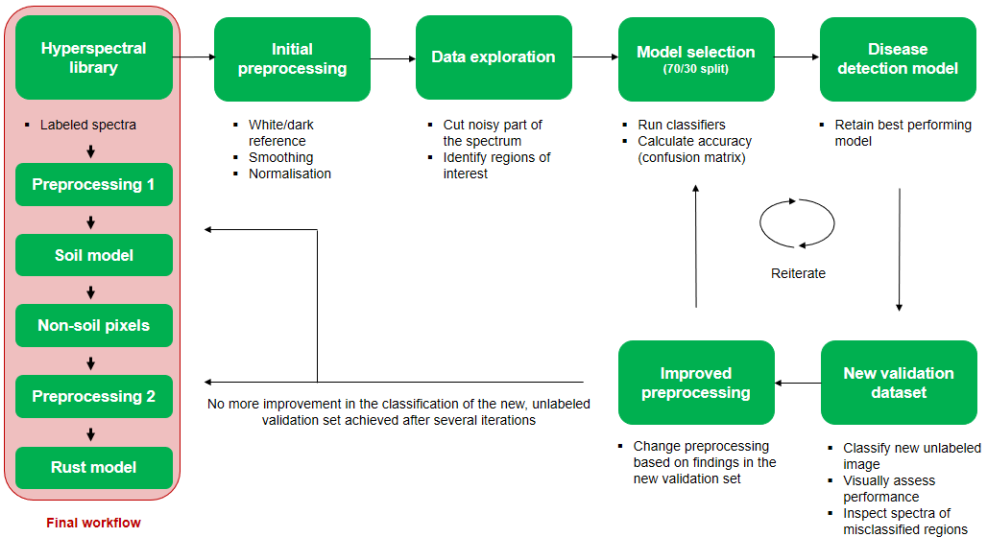

Figure 2: preprocessing and model selection cycle. The area highlighted in the leftmost square box with wording 'Final workflow' represents the final workflow. The rest of the chart represents the steps taken to determine this final workflow.

2.5. Leek rust disease

For leek rust disease, this resulted in a final disease detection workflow containing two models, one for soil and background classification and one for leek rust disease classification. Each of these models had its proper preprocessing step, marked as "preprocessing 1" and "preprocessing 2" in Figure 2. Preprocessing 1 included white/dark reference correction, Savitzky-Golay smoothing algorithm (window 33, polyorder 2), cutting wavebands before 445 nm and after 914 nm, and first derivation. This dataset was then used as input for the soil classification model. The feature used was the 702 nm band of the first derivative spectrum. The model used was a standard LDA algorithm (Pedregosa et al. 2011). Other soil classification strategies such as using normalized difference vegetation index (NDVI) values were also assessed. The result of the soil classification was used to retain only crop and disease pixels for further modelling. The dataset was then subjected to preprocessing 2. This included white/dark reference correction, Savitzky-Golay smoothing algorithm (window 33, polyorder 2), cutting wavebands before 445 nm and after 914 nm, normalisation (range between 0 and 1), and first derivation.

Certain rust spectra in the hyperspectral library with a low reflection (below 0.13) in the 661 nm waveband showed misclassification issues. Because reflection in the 661 nm band was observed to typically be high in rust pustule pixels, the training labels of these pixels were changed from 'rust' to 'weed'. This reduced misclassification by teaching the model to associate only high reflectance in this waveband with rust disease.

Three features were selected from this dataset: reflectance values at 556 and 661 nm and the value of the first derivative at 511 nm.

The model used to identify diseased pixels was a logistic regression model with class weights 0.4 for rust, 1 for healthy leek tissue and 1 for weeds. The LogisticRegressionCV function was used to automatically optimize the C-value parameter, given seven possible values as input (0.1, 0.5, 1, 1.5, 2, 4, 10). A C value of 0.5 was retained. During modelling, 70% of the dataset was used for model training and 30% (randomly selected) was used for model validation.

2.6. Leek white tip disease

The final white tip disease detection workflow contained two models, one for soil and background classification and one for disease classification, each with its own preprocessing strategy. The first preprocessing steps were the same for both soil and disease classification and consisted of: white/dark reference correction, Savitzky-Golay smoothing (window 33, polyorder 2), and min-max normalisation (between 0 and 1), similar to the leek rust disease model. Then, LDA classification was used to distinguish soil from non-soil pixels using the full spectrum as an input. Other soil classification strategies such as using normalized difference vegetation index (NDVI) values were also assessed.The presence of vertical striped noise, interfered with soil classification in the leek white tip disease dataset. A noise removal algorithm was built to remove this noise, by iteratively checking each linescan for noisy pixels and setting their classification result equal to neighbouring pixels.

Since white tip disease causes widespread damage on the leaf surface, it is expected that the pathogen is present in the green tissue surrounding white lesions, before visible symptoms appear. To examine this characteristic of the disease, a cross-section of pixels over a white tip lesion was plotted to examine the development of the spectral signature from healthy to highly diseased. Based on this cross-section, it was observed that the 594 nm band (and surrounding bands) varied greatly as disease progressed. The training data was therefore divided into four training datasets containing the full spectrum, based on the reflection in the 594 nm band: reflectance between 0 and 0.2 = ‘early disease’, between 0.2 and 0.4 = ‘moderate disease progression’, 0.4 to 0.6 = ‘severe disease progression’ and reflectance greater than 0.6 = ‘fully diseased. This dataset was then subjected to LDA transformation, which performed best out of all dimensionality reduction techniques. This reduced the dataset to four features, which was then used as input for a logistic regression algorithm to classify different disease stages from healthy leek tissue (Pedregosa et al. 2011). The LogisticRegressionCV function was used to automatically optimize the C-value parameter, given seven possible values as input (0.1, 0.5, 1, 1.5, 2, 4, 10). A C-value of 0.5 was retained. 70% of the dataset was used for model training and 30% (randomly selected) was used for model validation.

3. Results

Figures 3 and 4 show the spectral signatures of leek rust disease and leek white tip disease, respectively.

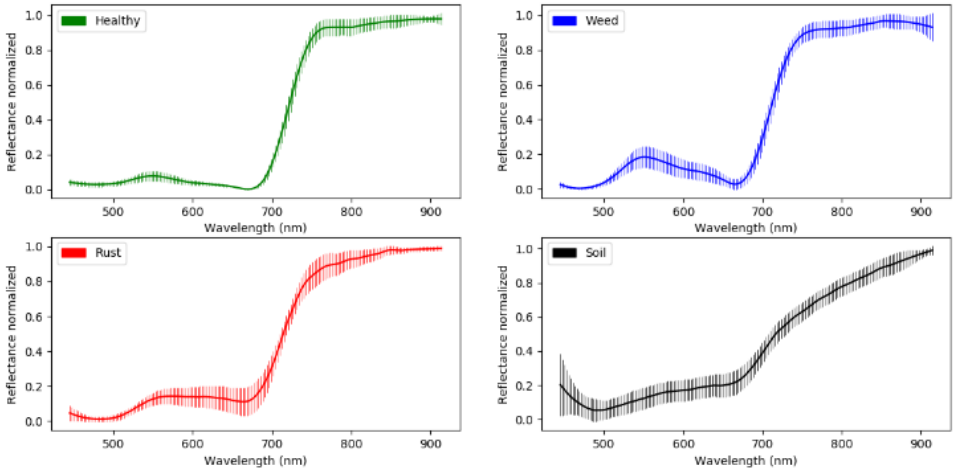

Figure 3: average reflectance curve for each of the four data classes included in the hyperspectral training library, after preprocessing. Error bars show standard deviation, giving an indication of the variability of the data per waveband and per class.

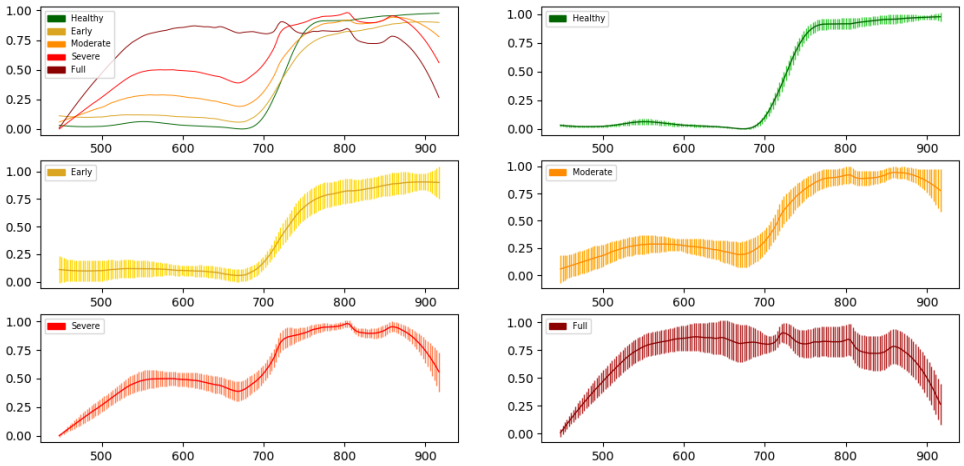

Figure 4: development of the average hyperspectral signature of leek white tip disease from early symptoms to fully diseased lesion. Training data was separated into four disease categories (early, moderate, severe, full) based on the reflectance of the 594 nm band. Spectra were subjected to Savitzky-Golay smoothing and min-max normalisation that scaled them between 0 and 1. X-axis shows wavebands (nm), y-axis shows relative reflectance.

3.1. Leek rust disease detection

The diagnostics of the soil classification model of the rust dataset were calculated based on the confusion matrix for the soil class (not shown), with 30% of the dataset reserved for model validation. Despite the soil classification model achieving a classification accuracy of 94.3%, the true positive rate was 1. This means that the 5.7% accuracy loss was due to misclassification of non-soil spectra, which is insignificant given that the only goal of this model is to accurately classify soil pixels.

Table 1 shows the diagnostics of the leek rust classification model, calculated based on the confusion matrix for the rust class (not shown), with 30% of the dataset reserved for model validation. The rust disease classification model showed an overall classification accuracy of 98.1%. The precision was 99%, meaning 99% of positive 'rust' disease classification results were accurate. This shows the model has been trained to be prone to 'miss' more rust spectra, but to have a high certainty that when a spectrum is classified as rust, it really is rust disease and not a false positive. This can be seen in the true positive rate that indicates that 84.4% of condition positives were correctly classified. The true negative on the other hand was 99.9%, indicating that 99.9% of the condition negatives were correctly classified.

Table 1: Diagnostics based on the confusion matrix (not shown) for the leek logistic regression rust detection model, trained using the reflectance value at 556 and 661 nm and the value of the first derivative at 511 nm. Class weights were set to 0.4 for rust, 1 for healthy and 1 for weeds. The training set was randomly split with a 70/30 ratio for training/validation.

Precision (%)	99%	True pos. rate	84.4%
Accuracy (%)	98.1%	False pos. rate	0.10%
PLR*	812.780	False neg. rate	15.58%
F1 score	0.9115	True neg. rate	99.90%

* PLR = Positive Likelihood Ratio

3.2. Leek white tip disease detection

Since the leek white tip disease model aimed at detecting different stages of disease, the model diagnostics based on the confusion matrix (not shown) have been calculated for each class separately (Table 2). The final classification accuracy of the leek white tip disease detection model was 96.74%. No confusion matrix or diagnostics are shown for the soil classification model. A soil segmentation model had to be chosen that would not affect phytophthora lesions (which show low NDVI, for example). For this reason, there was striped noise in the classified image that had to be removed by a custom-built filter algorithm.

Table 2: diagnostics of the white tip disease detection model derived from the confusion matrix for the results obtained by means of the logistic regression model.

	TPR	**TNR**	**PPV**	**NPV**	**FPR**	**FNR**	**FDR**	**ACC**
Healthy	99.23	96.41	98.19	98.46	3.59	0.77	1.81	98.28
Early	91.00	98.68	93.92	98.00	1.32	9.00	6.08	97.28
Moderate	86.57	99.21	87.44	99.14	0.79	13.43	12.56	98.45
Severe	88.41	99.89	95.39	99.71	0.11	11.59	4.61	99.61
Full	99.79	99.87	98.32	99.98	0.13	0.21	1.68	99.87

*TPR = true positive rate, TNR = true negative rate, PPV = positive predictive value, NPV = negative predictive value, FPR = false positive rate, FNR = false negative rate, FDR = false discovery rate, ACC = accuracy

3.3. Classification of field images

Figure 5 shows a classified image of the leek rust disease. Figure 5A shows the hyperspectral image (RGB representation from the hypercube). Figure 5B shows the classified hyperspectral image. Note that the model was trained specifically to be precise in classifying rust pixels, causing significant misclassifications in weeds vs. healthy leek tissue. Figures 6C and 6D show a close-up of rust pustules with a dimension of 2 mm^2 that have been detected by the model.

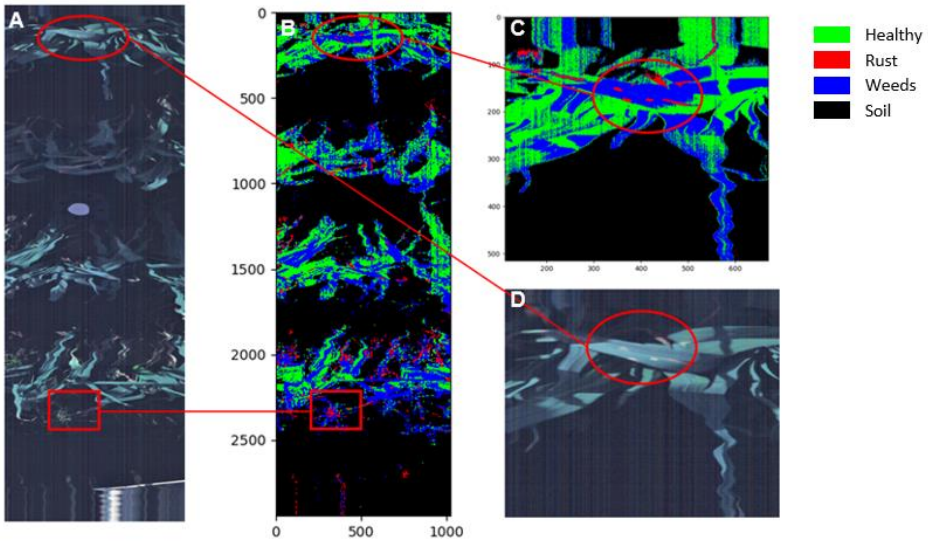

Figure 5: classification of a hyperspectral field image using the soil and leek rust classification models. Red, green, blue (RGB) images shown (A, D) corresponding to the full classified image (B) and a close-up (C). Circles indicate a typical rust infected leaf. Rectangle corresponds to a weed plant that appeared to contain rust disease after classification.

Figure 6 shows the final disease detection workflow. First, soil classification was used to segment the image (Figure 6B). The result was subject to striped noise, which was misclassified as 'crop'. This was solved by a custom noise filter (Figure 6C). Figure 6D shows a close-up of the classified image, showing the concentric pattern of the disease as it spread through the leaf from the initial infection site.

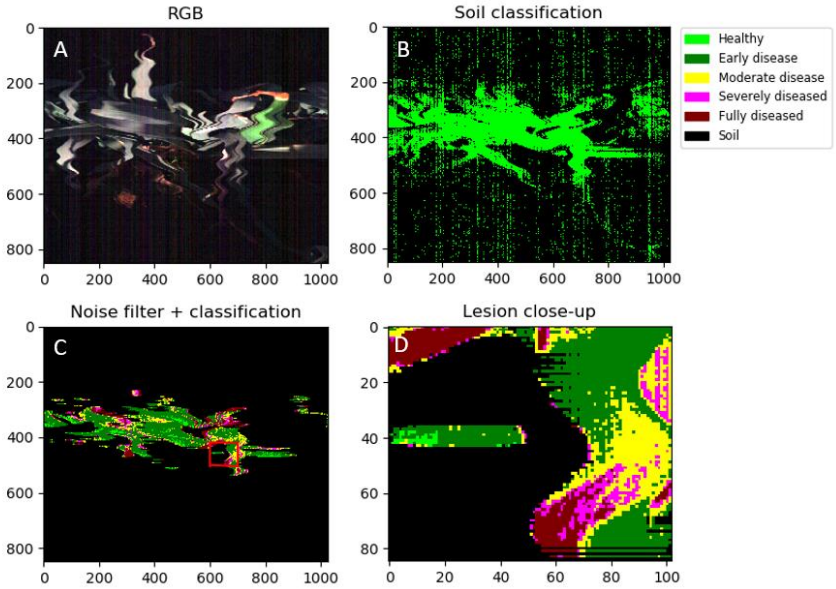

Figure 6: classification of a hyperspectral image of infected leek plants with white tip disease. X and Y axis values represent pixels (0.4 mm pixel size). RGB image is shown as a visual reference for disease severity (A). The soil classification step is shown, exhibiting striped noise (B). This was solved by a noise filter, after which classification was done (C). A close-up of the classified lesion in the red square area is shown with pre-visible disease detection (D).

4. Discussion

Comparing to literature, there is an absence of available works on hyperspectral-based leek white tip and rust disease detection. It was therefore necessary to compare the classification of the current work with rust or phytophthora diseases on other crops. White tip disease causes more extensive tissue damage ,spreading throughout the leaf, while leek rust disease produces small pustules for

propagation, rather than growing throughout the leaf surface. Extensive leave damage opens perspectives for early, pre-symptomatic disease detection before damage becomes visible to the human eye. For leek rust disease, early detection could be considered detecting single rust pustules, as this is the start of infection and causes relatively negligible damage to the crop. Comparing accuracy of disease detection, the leek rust model and white tip disease models perform comparably, with 98.14% and 96.74%, respectively. It needs to be noted however that the overall classification accuracy of the leek white tip model is less significant as an indicator of model performance in the context of variable rate fungicide applications since it is based on 4 disease classes. For these applications, fungicides will be applied as soon as disease is found in any stage of development, making the true negative rate (TNR) of the healthy class a more interesting statistic, because the TNR signifies the ability to detect 'healthy' negative – i.e. 'diseased' – spectra in the population. For this model, the TNR of 96.41% means that only 3.59% of diseased pixels (regardless of the disease stage) were identified as 'healthy'. Modelling the spread of disease throughout the crop in four disease classes is still useful, since it gives an indication on the growth pattern of the disease, and whether the pathogen is still actively growing.

For hyperspectral detection of rust diseases, a large amount of work has been done by authors working on winter wheat (Moshou et al. 2005; Whetton et al. 2018; Whetton, Waine, and Mouazen 2018; Bock et al. 2010; L. S. Huang et al. 2015). Huang et al. (2015) used reflectance in the 704, 1423 and 1926 nm bands to assess yellow rust severity on detached leaves with a coefficient of determination of 88% (L. S. Huang et al. 2015). Zhou et al. (2016) used two wavebands (558 nm and 856 nm) to classify yellow rust disease with an accuracy of 90.6%. Moshou et al. (2005) fused hyperspectral data in the 450 – 900 nm range with fluorescence imaging to detect yellow rust with an accuracy of 94.5%. These results show that the classification accuracy of leek rust disease of 98.14% in the current work appears to be promising and comparable to other rust diseases. The fact that it was possible to detect single rust pustules (Figure 5), means there is potential for identifying early rust infections and therefore possibly variable rate fungicide applications. Moreover, the fact that only three features were used in the current work (556 and 661 nm and the value of the first derivative at 511 nm), all of which are located in the green and red colour region, indicates a potential to replace costly hyperspectral cameras with cheaper multispectral or even RGB cameras. This is in line with findings by Zhou et al. (2015), who were able to detect yellow rust on wheat using RGB cameras at 74% and 81% accuracy (Zhou et al. 2015). The fact that mainly the green and red regions appear interesting for rust disease detection seems logical, given the red appearance of rust pustules. This shows the disadvantage of the LDA transformation that was used to classify white tip disease, whereby the features used can no longer be interpreted.

Hyperspectral detection of *Phytophthora* diseases on other crops than leek has received more attention in literature, with special interest for early disease detection (Franceschini et al. 2019, 2017; Gold et al. 2020; Rumpf et al. 2010; Xie et al. 2015; Fernández et al. 2020). Gold et al. (2020) for example report classification accuracies near 80% for *P. infestans* on potato, depending on the disease stage. However, these results were obtained in laboratory conditions. Fernandez *et al.* (2020) made a notable effort with a classification accuracy of 91.11% on infected potato leaves in controlled conditions. These works achieved disease detection in early conditions, but were executed under laboratory conditions. It is well-described in literature that the transference of disease detection data from laboratory to field conditions can be challenging (Behmann et al. 2015; Bohnenkamp, Behmann, and Mahlein 2019; A.-K. Mahlein et al. 2018; Mishra et al. 2017; Paulus and Mahlein 2020). Comparing these results to the leek white tip disease detection presented in the current work, the accuracy of 96.74% seems promising towards variable rate fungicide applications, given that it was obtained in field conditions.

5. Conclusions

The results presented in this work show that there is potential for early, pre-symptomatic detection of leek white tip disease with a classification accuracy of 96.74%. Detection of leek rust disease is also promising, with a classification accuracy of 98.14%, although no early disease detection was possible. The biggest challenge for variable rate fungicide applications lies in the development of a practical method to use these models in field conditions. Both data processing and storage needs are a concern, as well as image and spatial resolution. Further studies should focus on exploring the best methods to apply the disease detection models in this work to field conditions, focusing on a environmental and economic cost-benefit. Future experiments should focus on mapping the spread of disease in commercial fields, adapting crop management strategies and then performing a cost-benefit analysis for the farmer and the environment. Trials in controlled conditions could additionally be beneficial to study early, pre-visible disease progression using this model. Finally, the possibility of expanding the results of disease detection in leek to other allium crops, like garlic and onion, is poorly explored and could provide insights towards creating a more universally applicable disease detection model.

Acknowledgements

Apart from the people listed on this paper, a big thanks to the people at Bottelare experimental farm, UGent mechanical workshop, the people from the 'Provinciaal Proefcentrum voor de Groenteteelt Oost-Vlaanderen' and colleagues who helped during field work.

References

1. Appeltans, S., A. Guerrero, S. Nawar, J. Pieters, and A.M. Mouazen. 2020. "Practical Recommendations for Hyperspectral and Thermal Proximal Disease Sensing in Potato And." *Remote Sensing* 12, 1939.: 1–19. https://doi.org/10.3390/rs12121939.
2. Archbold Taylor, George, Hector Beltran Torres, Fredy Ruiz, Margarita Narducci Marin, DIego Mendez Chaves, Luis Trujillo Arboleda, Carlos Parra, Henry Carrillo, and Abdul M. Mouazen. 2019. "PH Measurement IoT System for Precision Agriculture Applications." *IEEE Latin America Transactions*. https://doi.org/10.1109/TLA.2019.8891951.
3. Behmann, Jan, Anne Katrin Mahlein, Till Rumpf, Christoph Römer, and Lutz Plümer. 2015. "A Review of Advanced Machine Learning Methods for the Detection of Biotic Stress in Precision Crop Protection." *Precision Agriculture* 16 (3): 239–60. https://doi.org/10.1007/s11119-014-9372-7.

4. Bock, C. H., G. H. Poole, P. E. Parker, and T. R. Gottwald. 2010. "Plant Disease Severity Estimated Visually, by Digital Photography and Image Analysis, and by Hyperspectral Imaging." *Critical Reviews in Plant Sciences* 29 (2): 59–107. https://doi.org/10.1080/07352681003617285.
5. Bohnenkamp, David, Jan Behmann, and Anne Katrin Mahlein. 2019. "In-Field Detection of Yellow Rust in Wheat on the Ground Canopy and UAV Scale." *Remote Sensing* 11 (21). https://doi.org/10.3390/rs11212495.
6. Clarkson, J. P., R. Kennedy, K. Phelps, J. Davies, and J. Bowtell. 1997. "Quantifying the Effect of Reduced Doses of Propiconazole (Tilt) and Initial Disease Incidence on Leek Rust Development." *Plant Pathology* 46 (6): 952–63. https://doi.org/10.1046/j.1365-3059.1997.d01-82.x.
7. Declercq, Bart, Jasper Devlamynck, David de Vleesschauwer, Nathalie Cap, Joris de Nies, Sabien Pollet, and Monica Höfte. 2012. "New Insights in the Life Cycle and Epidemics of Phytophthora Porri on Leek." *Journal of Phytopathology* 160 (2): 67–75. https://doi.org/10.1111/j.1439-0434.2011.01860.x.
8. Doherty, Maureen A., and T. F. Preece. 1978. "Bacillus Cereus Prevents Germination of Uredospores of Puccinia Allii and the Development of Rust Disease of Leek, Allium Porrum, in Controlled Environments." *Physiological Plant Pathology* 12 (1): 123–32. https://doi.org/10.1016/0048-4059(78)90025-5.
9. Fernández, Claudio Ignacio, Brigitte Leblon, Ata Haddadi, Keri Wang, and Jinfei Wang. 2020. "Potato Late Blight Detection at the Leaf and Canopy Levels Based in the Red and Red-Edge Spectral Regions." *Remote Sensing*. https://doi.org/10.3390/RS12081292.
10. Franceschini, Marston Héracles Domingues, Harm Bartholomeus, Dirk Frederik van Apeldoorn, Juha Suomalainen, and Lammert Kooistra. 2019. "Feasibility of Unmanned Aerial Vehicle Optical Imagery for Early Detection and Severity Assessment of Late Blight in Potato." *Remote Sensing*. https://doi.org/10.3390/rs11030224.
11. Franceschini, Marston Héracles Domingues, Harm Bartholomeus, Dirk van Apeldoorn, Juha Suomalainen, and Lammert Kooistra. 2017. "Intercomparison of Unmanned Aerial Vehicle and Ground-Based Narrow Band Spectrometers Applied to Crop Trait Monitoring in Organic Potato Production." *Sensors (Switzerland)* 17 (6). https://doi.org/10.3390/s17061428.
12. Geiger, Flavia, Jan Bengtsson, Frank Berendse, Wolfgang W. Weisser, Mark Emmerson, Manuel B. Morales, Piotr Ceryngier, et al. 2010. "Persistent Negative Effects of Pesticides on Biodiversity and Biological Control Potential on European Farmland." *Basic and Applied Ecology*. https://doi.org/10.1016/j.baae.2009.12.001.
13. Gold, Kaitlin M., Philip A. Townsend, Adam Chlus, Ittai Herrmann, John J. Couture, Eric R. Larson, and Amanda J. Gevens. 2020. "Hyperspectral Measurements Enable Pre-Symptomatic Detection and Differentiation of Contrasting Physiological Effects of Late Blight and Early Blight in Potato." *Remote Sensing* 12 (2). https://doi.org/10.3390/rs12020286.
14. Grisham, Michael P., Richard M. Johnson, and Paul V. Zimba. 2010. "Detecting Sugarcane Yellow Leaf Virus Infection in Asymptomatic Leaves with Hyperspectral Remote Sensing and Associated Leaf Pigment Changes." *Journal of Virological Methods*. https://doi.org/10.1016/j.jviromet.2010.03.024.
15. Heaton, Jeff. 2016. "An Empirical Analysis of Feature Engineering for Predictive Modeling." In *Conference Proceedings - IEEE SOUTHEASTCON*. https://doi.org/10.1109/SECON.2016.7506650.
16. Huang, Lin Sheng, Shu Cun Ju, Jin Ling Zhao, Dong Yan Zhang, Qi Hong, Ling Teng, Fan Yang, and Yan Zuo. 2015. "Hyperspectral Measurements for Estimating Vertical Infection of Yellow Rust on Winter Wheat Plant." *International Journal of Agriculture and Biology* 17 (6). https://doi.org/10.17957/IJAB/15.0034.
17. Jennings, D. M., B. V. Ford-lloyd, and G. M. Butler. 1990. "Effect of Plant Age, Leaf Position and Leaf Segment on Infection of Leek by Leek Rust, Puccinia Allii." *Plant Pathology*. https://doi.org/10.1111/j.1365-3059.1990.tb02538.x.
18. Jong, P. D. de, R. A. Daamen, and R. Rabbinge. 1995. "The Reduction of Chemical Control of Leek Rust, a Simulation Study." *European Journal of Plant Pathology* 101 (6): 687–93. https://doi.org/10.1007/BF01874873.
19. Mahlein, A.-K., M.T. Kuska, J. Behmann, G. Polder, and A. Walter. 2018. "Hyperspectral Sensors and Imaging Technologies in Phytopathology: State of the Art." *Annual Review of Phytopathology* 56 (1): 535–58. https://doi.org/10.1146/annurev-phyto-080417-050100.
20. Mahlein, Anne-Katrin. 2016. "Plant Disease Detection by Imaging Sensors - Parallels and Specific Demands for Precision Agriculture and Plant Phenotyping." *Plant Disease* 100 (2): 1–11. https://doi.org/10.1007/s13398-014-0173-7.2.
21. Mishra, Puneet, Mohd Shahrimie Mohd Asaari, Ana Herrero-Langreo, Santosh Lohumi, Belén Diezma, and Paul Scheunders. 2017. "Close Range Hyperspectral Imaging of Plants: A Review." *Biosystems Engineering*. https://doi.org/10.1016/j.biosystemseng.2017.09.009.
22. Moshou, D., C. Bravo, R. Oberti, J. West, L. Bodria, A. McCartney, and H. Ramon. 2005. "Plant Disease Detection Based on Data Fusion of Hyper-Spectral and Multi-Spectral Fluorescence Imaging Using Kohonen Maps." *Real-Time Imaging* 11 (2): 75–83. https://doi.org/10.1016/j.rti.2005.03.003.
23. Nawar, Said, Ronald Corstanje, Graham Halcro, David Mulla, and Abdul M. Mouazen. 2017. *Delineation of Soil Management Zones for Variable-Rate Fertilization: A Review. Advances in Agronomy*. Vol. 143. https://doi.org/10.1016/bs.agron.2017.01.003.
24. Paulus, Stefan, and Anne Katrin Mahlein. 2020. "Technical Workflows for Hyperspectral Plant Image Assessment and Processing on the Greenhouse and Laboratory Scale." *GigaScience*. https://doi.org/10.1093/gigascience/giaa090.
25. Pedregosa et al. 2011. "Scikit-Learn: Machine Learning in Python." *JMLR 12*, 2825–30.
26. Rumpf, T., A. K. Mahlein, U. Steiner, E. C. Oerke, H. W. Dehne, and L. Plümer. 2010. "Early Detection and Classification of Plant Diseases with Support Vector Machines Based on Hyperspectral Reflectance." *Computers and Electronics in Agriculture* 74 (1): 91–99. https://doi.org/10.1016/j.compag.2010.06.009.
27. Smith, B M, T C Crowther, J P Clarkson, and L Trueman. 2000. "Partial Resistance to Rust (Puccinia Allii) in Cultivated Leek (Allium Ampeloprasum Ssp.Porrum): Estimation and Improvement." *Annals of Applied Biology* 137 (1): 43–51. https://doi.org/10.1111/j.1744-7348.2000.tb00055.x.

28. Theunissen, J., and G. Schelling. 1996. “Pest and Disease Management by Intercropping: Suppression of Thrips and Rust in Leek.” *International Journal of Pest Management* 42 (4): 227–34. https://doi.org/10.1080/09670879609372000.
29. Whetton, Rebecca L., Kirsty L. Hassall, Toby W. Waine, and Abdul M. Mouazen. 2018. “Hyperspectral Measurements of Yellow Rust and Fusarium Head Blight in Cereal Crops: Part 1: Laboratory Study.” *Biosystems Engineering* 166: 101–15. https://doi.org/10.1016/j.biosystemseng.2017.11.008.
30. Whetton, Rebecca L., Toby W. Waine, and Abdul M. Mouazen. 2018. “Hyperspectral Measurements of Yellow Rust and Fusarium Head Blight in Cereal Crops: Part 2: On-Line Field Measurement.” *Biosystems Engineering* 167: 144–58. https://doi.org/10.1016/j.biosystemseng.2018.01.004.
31. Xie, Chuanqi, Yongni Shao, Xiaoli Li, and Yong He. 2015. “Detection of Early Blight and Late Blight Diseases on Tomato Leaves Using Hyperspectral Imaging.” *Scientific Reports* 5: 1–11. https://doi.org/10.1038/srep16564.
32. Zhang, Jingcheng, Y. Huang, Ruiliang Pu, P. Gonzalez-Moreno, Lin Yuan, Kaihua Wu, and Wenjiang Huang. 2019. “Monitoring Plant Diseases and Pests through Remote Sensing Technology: A Review.” *Computers and Electronics in Agriculture*. https://doi.org/10.1016/j.compag.2019.104943.
33. Zhang, Jingcheng, Ruiliang Pu, Wenjiang Huang, Lin Yuan, Juhua Luo, and Jihua Wang. 2012. “Using In-Situ Hyperspectral Data for Detecting and Discriminating Yellow Rust Disease from Nutrient Stresses.” *Field Crops Research*. https://doi.org/10.1016/j.fcr.2012.05.011.
34. Zhou, B., A. Elazab, J. Bort, O. Vergara, M. D. Serret, and J. L. Araus. 2015. “Low-Cost Assessment of Wheat Resistance to Yellow Rust through Conventional RGB Images.” *Computers and Electronics in Agriculture* 116. https://doi.org/10.1016/j.compag.2015.05.017.